Journal of Applied Electrochemistry **30**: 647–656, 2000.

Regeneration of zinc particles for zinc–air fuel cells in a spouted-bed electrode

V. JIRICNY[1], S. SIU[2], A. ROY[2] and J.W. EVANS[2]*
[1]*Institute of Chemical Process Fundamentals, Prague, Czech Republic*
[2]*Department of Materials Science and Mineral Engineering, University of California, Berkeley, CA 94720, USA*
*(*author for correspondence)*

Received 1 March 1999; accepted in revised form 8 February 2000

Key words: fluidised bed, fuel cells, spouted bed, zinc–air, zinc electrowinning, zinc particles

Abstract

Fuel cells wherein zinc particles form a negative electrode and a gas-diffusion electrode (air electrode) is the positive electrode, are under development. Such cells are dependent on the regeneration of the zinc particles (and electrolyte). This paper describes experiments on electrolytic cells equipped with spouted bed cathodes for use in this application. Experiments have been carried out on laboratory scale cells to determine the operability of cells for growing 'seed' particles in the range from 0.4 to 1 mm to measure cell voltage and current efficiency (and thereby energy consumption rate), and to identify a suitable material that could be used as a diaphragm (separating the spouted bed from the oxygen evolving anode). A larger cell, capable of producing up to 10 kg Zn per day, was designed and built. The larger cell was run successfully fifteen times and showed cell voltages and energy consumption rates comparable with those of smaller cells.

1. Introduction

The topic of zinc–air batteries or fuel cells has recently been reviewed by Will [1]. In such cells the negative electrode is a zinc electrode in contact with a potassium hydroxide electrolyte; this electrode faces a positive gas diffusion electrode wherein oxygen reacts with the water of the electrolyte to produce hydroxyl ions. The oxygen is typically that of ambient air, perhaps with prior removal of carbon dioxide and humidification. Two categories of secondary zinc–air batteries are apparent: those that are electrically recharged and those where, after discharge, spent electrolyte is replaced with fresh electrolyte and fresh zinc. The latter are frequently known as mechanically recharged batteries, mechanically refuelled batteries or fuel cells and it is this last category that is relevant to the present study. Of particular interest is the regeneration of zinc particles for use in fuel cells of the type described by Savaskan and Evans [2, 3], Savaskan et al. [4], Salas and Evans [5], Cooper [6] and by Cooper and coworkers [7]. In these cells the zinc is in the form of particles (of the order of 1 mm in size) which are pumped into the cell in suspension in KOH electrolyte. The particles and fresh electrolyte must then be generated from spent electrolyte pumped from the cell at the end of discharge. The use of a fluidized-bed electrode for this regeneration step has been described by Huh et al. [8] but the electrical energy consumption was of the order of 2 kWh kg^{-1} of Zn, exclusive of pumping energy. The energy derived from the fuel cell is typically around 1 kWh kg^{-1} of Zn. Consequently, the efficiency of the whole system is only approximately 50%. An alternative approach was considered worthwhile and such an alternative is the spouted-bed electrode (SBE). The paper describes an investigation of the SBE in this application and includes some results for a large-scale cell capable of producing up to 10 kg per day of zinc.

2. Experiments with laboratory scale cells

2.1. *Apparatus and procedure*

In the early stages of this investigation a cell with a cylindrical spouted-bed cathode was tried. Because that cell was less successful than the rectangular ('flat') design described below, it is only mentioned here and the interested reader is referred to the literature [9]. The flat cell is depicted in Figure 1 where the upper drawing is a front view of the cathode and the lower drawing is an exploded view of the cell from above. The spouted bed of growing zinc particles lay in the cathode side of the cell on both sides of a central 'draft tube'. The inflow of catholyte, through a nozzle at the bottom of the cell, carried particles up the draft tube to form a fountain of particles at the top of the tube. The catholyte passed out of the cell through outlets at the top while the particles fell onto beds on either side of the draft tube. After descending through those beds the particles fell through

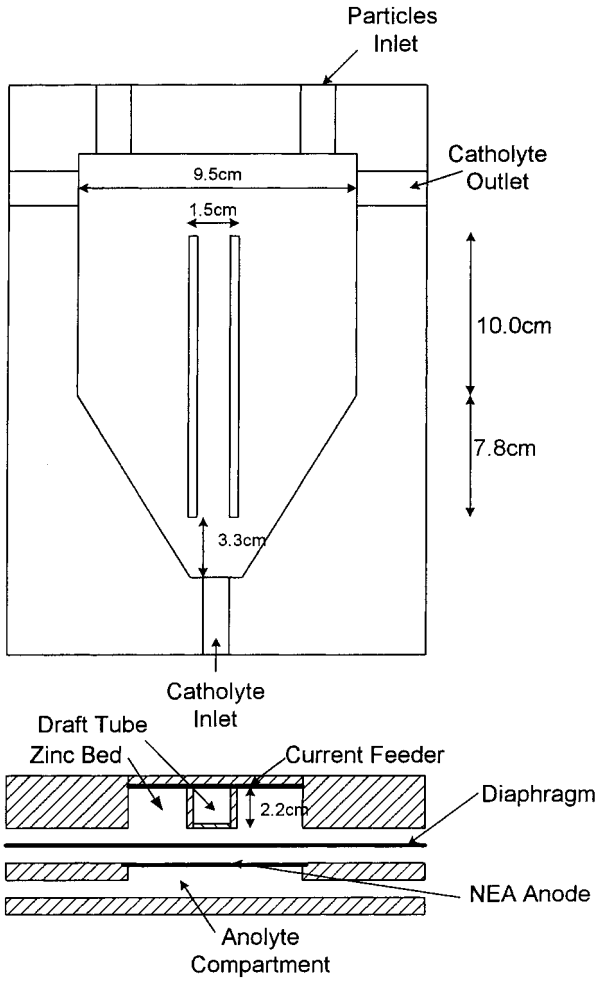

Fig. 1. Schematic diagram of the flat spouted bed cell.

a gap between the draft tube and the inclined wall and were again entrained in the catholyte passing up the tube. Spouted beds can be operated without draft tubes but in earlier studies [10, 11], on electrodeposition of zinc from acid sulfate electrolytes, a draft tube had been found to facilitate scale up of the cell in a vertical direction and to reduce the pressure at the bottom of the bed.

The spouted cathode was separated from the anode side of the cell by a porous diaphragm. An oxygen evolving anode (a nickel mesh with a proprietary coating that is catalytic for oxygen evolution, Electrolyser Corp., Toronto) was used and the electrical connections to the cell were to the top of the anode and to the top of a copper 'current feeder' located at the back of the spouted bed. Both anolyte and catholyte were pumped from separate reservoirs, through flowmeters and the cell, before returning to the reservoirs. The catholyte reservoir was connected to a hydrogen burette so that hydrogen evolution at the cathode (and thereby current efficiency) could be measured by measuring the mass of water displaced by any evolving hydrogen.

Batch operation was employed. A measured mass of zinc particles was placed in the cell, the reservoirs were filled with electrolyte (analytical grade reagents and distilled water) of the required concentration and the electrolytes brought up to the required temperature by circulating hot water through coils immersed in the reservoirs. The pumps were then turned on and, after proper spouting was observed, the d.c. power supply was switched on and adjusted to the required current. Electrolysis continued for the required period with hydrogen evolution, cell voltage and current monitored. Electrolyte temperature was controlled by circulating hot or cold water, as required, through the immersed coils. Afterwards the particles were removed from the cell and the cell disassembled.

2.2. *Experimental results*

Typical results from the cell of Figure 1 are shown in Figure 2 where cell voltage, current efficiency and energy consumption (calculated from the first two measurements) are plotted against the zinc concentration (calculated from the measured current efficiency). With separate electrolytes, hydrogen evolution is the phenomenon responsible for loss of current efficiency and measurement of hydrogen evolution served as a convenient way of monitoring current efficiency; its accuracy was checked by weighing the zinc after the experiment. The experiment of Figure 2 started with 30%, by weight, of KOH (prior to dissolution of zinc oxide) and the particles fed to the bed were 1.45 mm cut wire particles. These particles (Abrasive Materials Corp., Hillsdale, MI, USA) were roughly isometric cylinders. The current employed in the experiment was 1000 A m^{-2} of diaphragm with this material being the microporous Celgard 5550 (Hoechst–Celanese Corp., Charlotte, NC, USA). Breaks in the curves of Figure 2 correspond to adjustment of electrolyte volume by addition of water.

It is seen from Figure 2 that the current efficiency stays high until nearly all the zinc has been recovered from the catholyte. At this current density the electrical energy consumption (kWh kg^{-1} zinc) entailed in the zinc regeneration is pleasingly low; it should be contrasted with the about 3 kWh kg^{-1} at 500 A m^{-2} of the conventional electrowinning of zinc from acid sulfate electrolytes [12]. Rather similar results for a catholyte of 45% KOH (before ZnO dissolution) are shown in Figure 3. Some of the results of Figure 3 pertain to experiments where the anolyte was 30% KOH. The current efficiency is again seen to stay high, until low zinc concentrations are reached, and is, as expected, the same for both anolytes. The slightly lower cell voltage (and therefore energy consumption) with 30% KOH as the anolyte is due to the higher conductivity of this electrolyte.

Returning to experiments where both electrolytes are 30% KOH, Figure 4 displays the energy consumption for operation at different current densities. Naturally, the cell voltage and energy consumption increase with current density but the latter is mostly below 2 kWh kg^{-1} Zn, even at 2500 A m^{-2}.

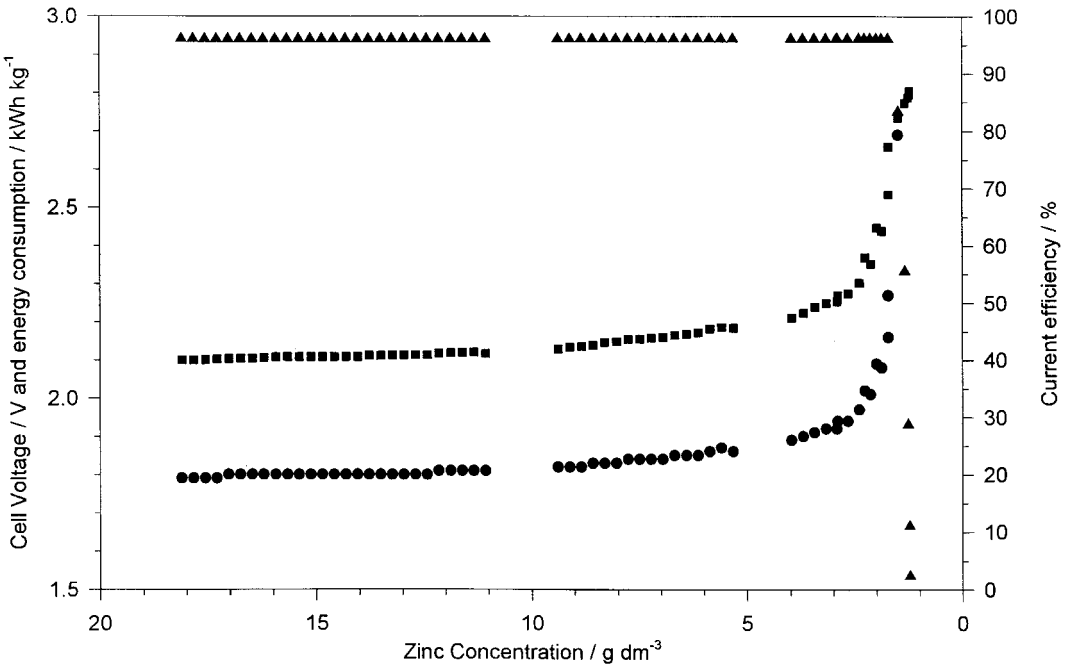

Fig. 2. Flat bed cell performance, 30 wt% KOH initially, 1.45 mm cut wire zinc particles, 35 °C. Key: (●) energy consumption, (■) cell voltage, (▲) current efficiency.

The experiments described so far were of a few hours duration. One long-term experiment was carried out to grow 0.4 mm cut wire particles (Platt Bros., Waterbury, CT, USA) to a final size of approximately 1 mm, that is, by a factor of approximately 17 in mass. Figure 5 illustrates the particles at various stages of growth, starting with the 0.4 mm seed particles; a 100 μm bar on each micrograph shows the size of the particles. The particles are seen to become more nearly spherical as they grow but to develop a rough surface. A cross section micrograph of a finished particle appears as Figure 6 and exhibits some porosity. The particles were found to flow freely, despite the surface roughness.

The long term experiment was successful in growing the particles substantially and in that a high current efficiency (98–100% by weight gain) was achieved. However, a major difficulty encountered in the long term was an upward drift of the cell voltage and thereby energy consumption. This is evident in Figure 7 where the consequences of changing from Celgard 5550 that had been used for some time to a fresh piece can be seen. The upward drift in energy consumption (cell

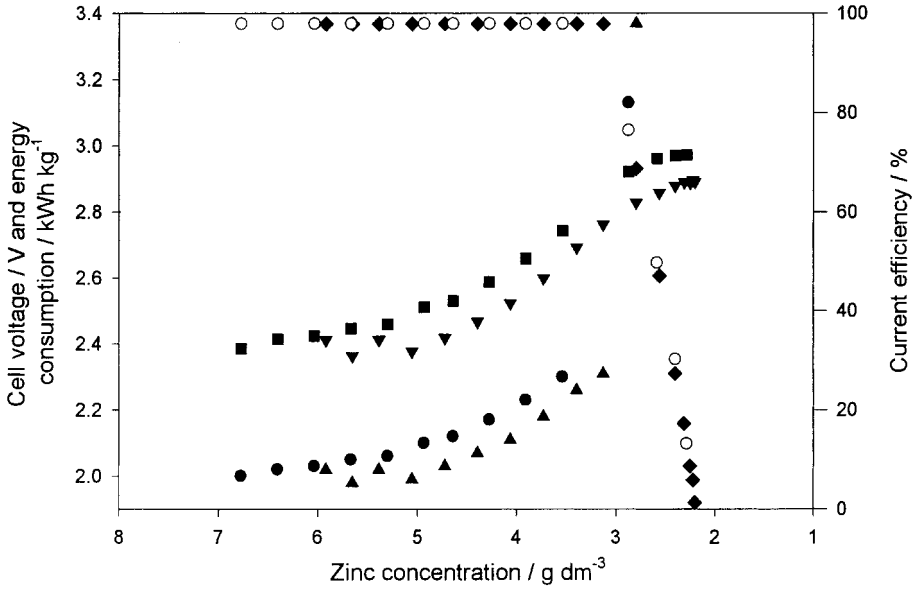

Fig. 3. Small cell performance with 45% KOH and 30% KOH anolyte; 1.45 mm cut wire zinc particles, 35 °C. Key: (●, ■, ○) energy consumption, cell voltage and current efficiency, respectively; (▲, ▼, ◆) energy consumption, cell voltage and current efficiency (30 wt% KOH anolyte), respectively.

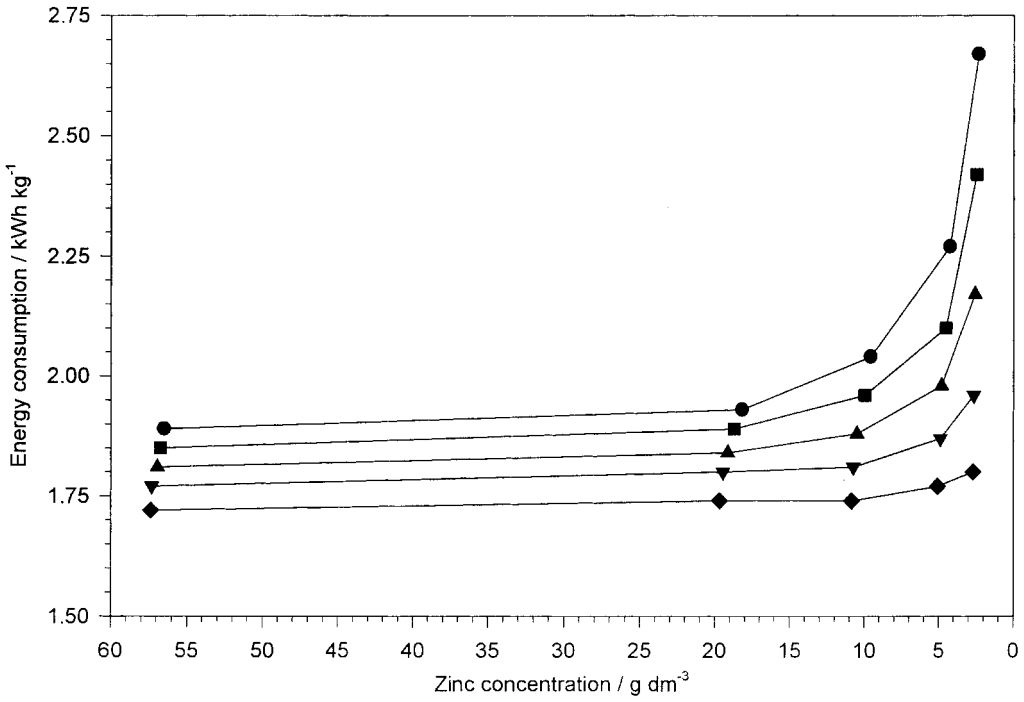

Fig. 4. Small cell performance at different current densities, 30 wt% KOH initially, 1.45 mm cut wire zinc particles, 35 °C. Key: (●) 2500, (■) 2000, (▲) 1500, (▼) 1000, (◆) 500 in A m^{-2}.

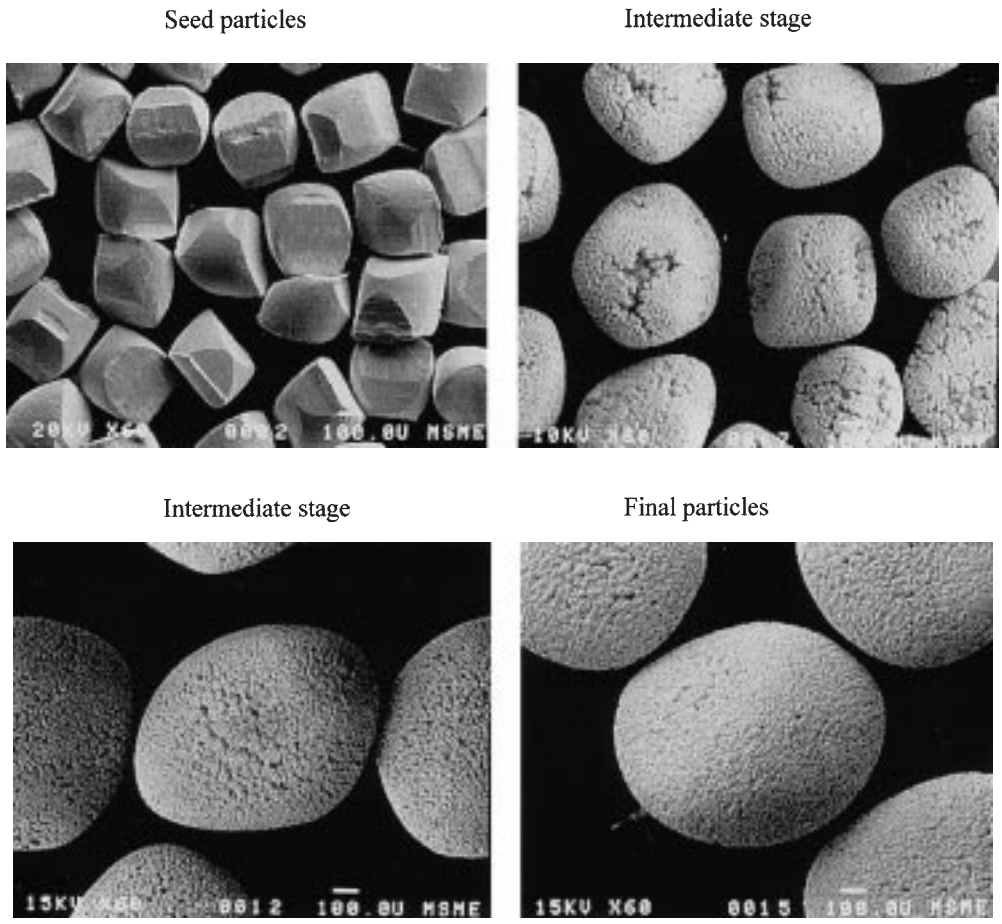

Fig. 5. SEM micrographs of zinc particles at different stages of growth.

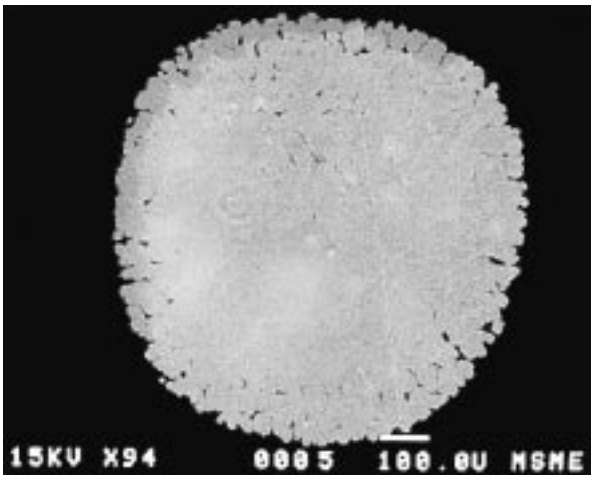

Fig. 6. SEM micrograph of cross section of a finished particle.

voltage) and the drop on changing the Celgard is explained as follows. Celgard incorporates a proprietary surfactant to promote wetting of this material by aqueous electrolytes. It was conjectured that this surfactant was leached from the Celgard by the flow of KOH on either side of the diaphragm, making it hydrophobic. Consequently, oxygen bubbles would become trapped between the Celgard and the anode, with which it is in contact, or within the pores of the Celgard, impeding the flow of current. The validity of this hypothesis was supported by the fact that regions of the Celgard exposed to the electrolyte in the cell were not wetted by water, whereas unexposed regions could still be wetted after an experiment. Therefore, an objective of subsequent investigation was a material that would remain hydrophilic.

Two materials that appeared to remain hydrophilic were a microporous polymeric material (E40201) from Pal RAI manufacturing Co. (Hauppauge, New York) and a more porous material (HS) from GC Processing (Rockland, DE, USA). The latter material, although quite permeable, appeared to be the stronger of the two materials while the former was much less permeable. Accordingly these materials were used in combination. The HS was in contact with the particles and the E40201, which the manufacturer describes as permanently hydrophylic, on the anode side of the combination. Figure 8 is a plot of the cell voltage and other variables during a batch experiment carried out at 1880 A m^{-2}. The stability of the voltage over the period of the experiment should be contrasted with the upward drift of the voltage in Figure 7. The specific productivity is the zinc deposition rate in kg zinc m^{-3} of bed of particles. The dependence of the cell voltage on cell current density is readily determined during the course of an experiment by ramping the current. Because such measurements are over in a few minutes, they are essentially performed at constant composition. Figure 9 gives the results for the experiment of Figure 8. The electrical energy consumption is seen to be below 2 kWh kg^{-1} Zn up to current densities of approximately 1500 A m^{-2}.

If a zinc–air fuel cell using particulate zinc and a recovery system using an SBE reach commercial application, it will be advisable to grow zinc particles over a broader range than the 0.4–1 mm range of the present investigation. For example, if particles can be grown from 0.1 to 1 mm, then the seed is 0.1% of the feed and is unlikely to burden the economics of zinc regeneration. With this in mind some experiments were con-

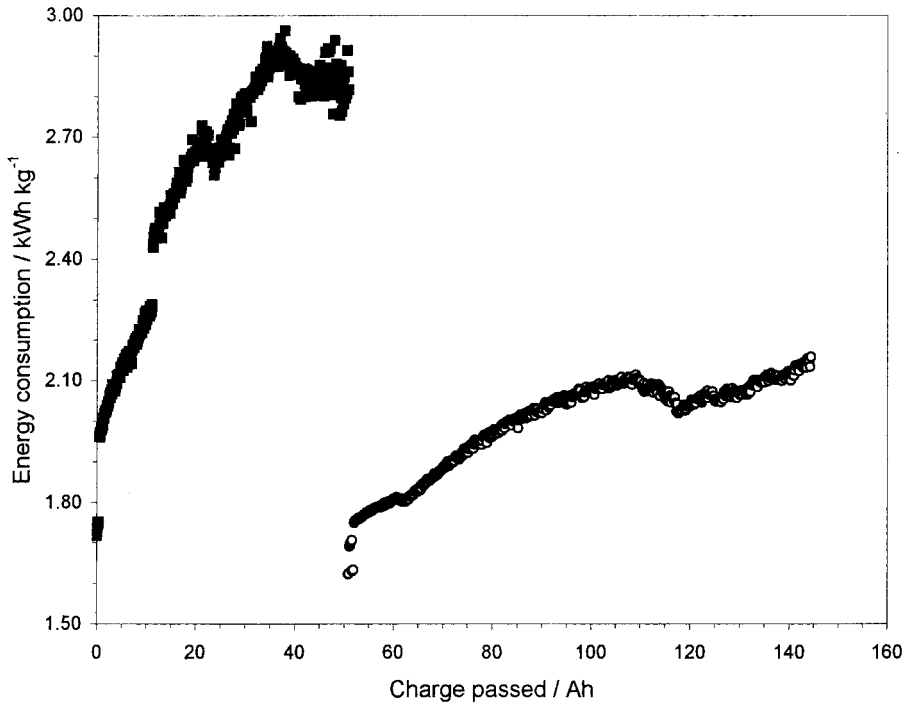

Fig. 7. Energy consumption with fresh and old Celgard in small cell, 40 °C, 2500 A m^{-2}. Key: (■) old Celgard, (○) fresh Celgard.

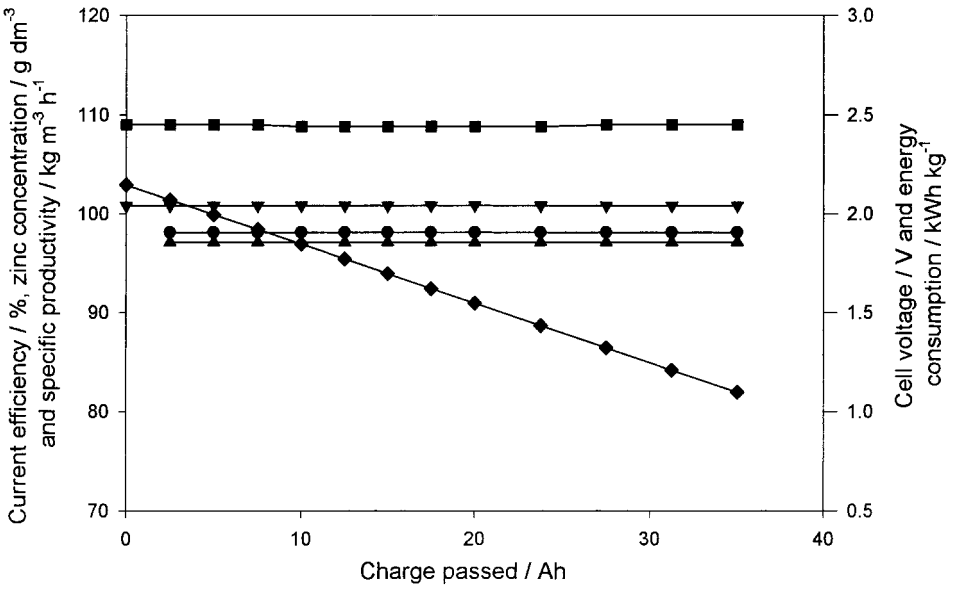

Fig. 8. Stability of cell voltage with time, 102.9 g dm^{-3} Zn in 45 wt% KOH, 1.5 dm^3, anolyte the same composition as catholyte, 0.5 dm^3, 40 °C, diaphragm E40201 and HS, 0.76 mm cut wire zinc particles, 1880 A m^{-2}. Key: (◆) zinc concentration, (▲) specific productivity, (●) current efficiency, (■) cell voltage and (▼) energy consumption.

ducted using samples of small particles from Union Miniere (Overpelt, Belgium). Particles from one of the samples are shown in Figure 10 and are seen to be smaller than the seed particles of Figure 5 but irregular in shape. This irregular shape resulted in the particles not flowing easily in the spouted bed and operation with these particles alone appeared impossible. However, in a continuously operated bed there would be a distribution of particle sizes. Consequently, an experiment with a mixture of small particles and larger particles is meaningful. Therefore, experiments were conducted with 90% (by mass) 0.4 mm cut wire particles and 10% Union Miniere particles. The cell was similar in design to that of Figure 1 (although taller) but included an expansion chamber at the top of the spouted bed to minimize elutriation of the finest particles. Daramic (a microporous polymeric material, Daramic Corp., Owensboro, KY, USA) was used as the diaphragm. Although unsuitable for long term use in alkaline electrolytes, the Daramic withstood cell conditions for a few hours without significant deterioration. Figure 11 gives experimental results for a run with this mixture of particle sizes. The electric energy consumption is seen to be only 1.8 kWh kg^{-1} and the cell was operated to a controlled shutdown (albeit after only a few hours).

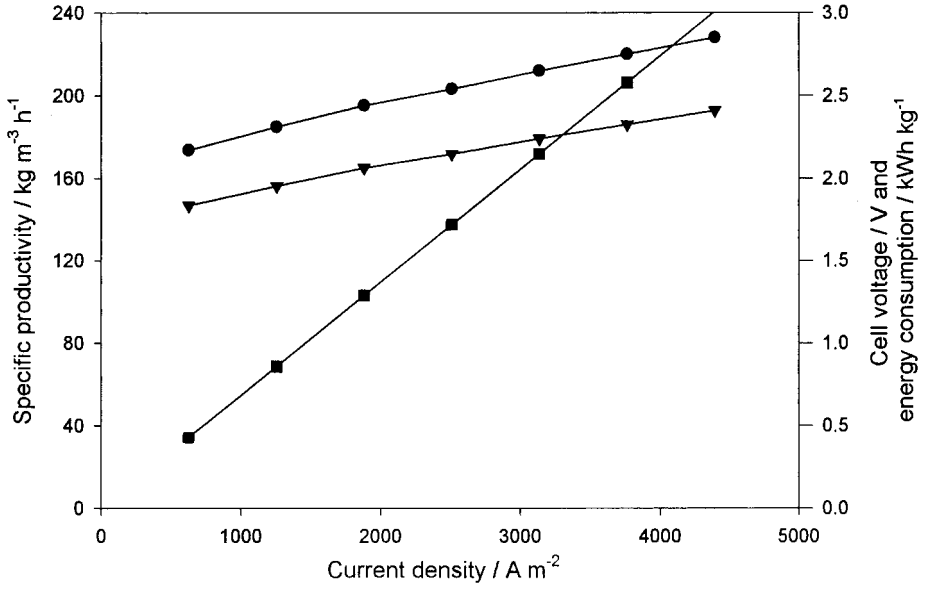

Fig. 9. Operational variables at different current densities; 102.9 g dm^{-3} zinc in 45 wt% KOH, 1.5 dm^3, anolyte the same composition as catholyte, 0.5 dm^3, 40 °C, diaphragm E40201 and HS, 0.76 mm particles. Key: (●) cell voltage, (▼) energy consumption and (■) specific productivity.

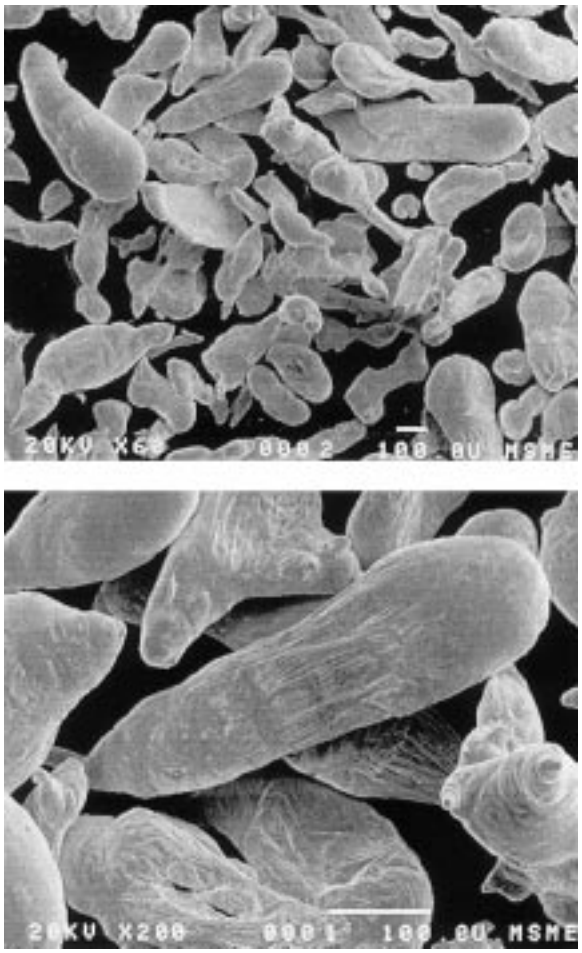

Fig. 10. SEM micrographs of zinc powder sample 2 from Union Miniere, SA, Belgium, in as-received condition.

3. Experiments with a larger cell

3.1. *Apparatus and procedure*

The larger cell was intended to produce 5 kg of zinc per 24 h, at a design current of 175 A, with the expectation that it could be operated at more than double that current (and production rate) without excessive energy consumption. The cell is illustrated in Figure 12; apart from the obvious greater size and the use of two draft tubes, the cell has another important difference from that of Figure 1. As seen in the latter Figure, a particle travelling down through the bed at the side away from the draft tube, in the smaller cell, encounters a change of slope, from vertical to 60° to the horizontal. The sudden change of slope is eliminated in Figure 12. Experience had taught that, if the particle flow displayed stagnant regions, those regions occurred at the change of slope. The cell was also designed with an expansion chamber above the bed so as to minimize any particle elutriation. The bed of particles was 23 mm thick; other dimensions and details can be found in Table 1.

The cell was operated in a batch manner using only one electrolyte reservoir. Electrolyte was pumped from the reservoir through flowmeters to both anode and cathode sides of the cell. The reservoir was open to the atmosphere; uptake of carbon dioxide was assumed too small to warrant closing the reservoir. The combination diaphragm of E40201 and HS, described above, was used, along with Electrolyser anodes.

The experimental procedure was similar to that described above for the laboratory scale cells (except for the absence of measurement of hydrogen evolution). Briefly, particles were placed in the cell, the electrolyte

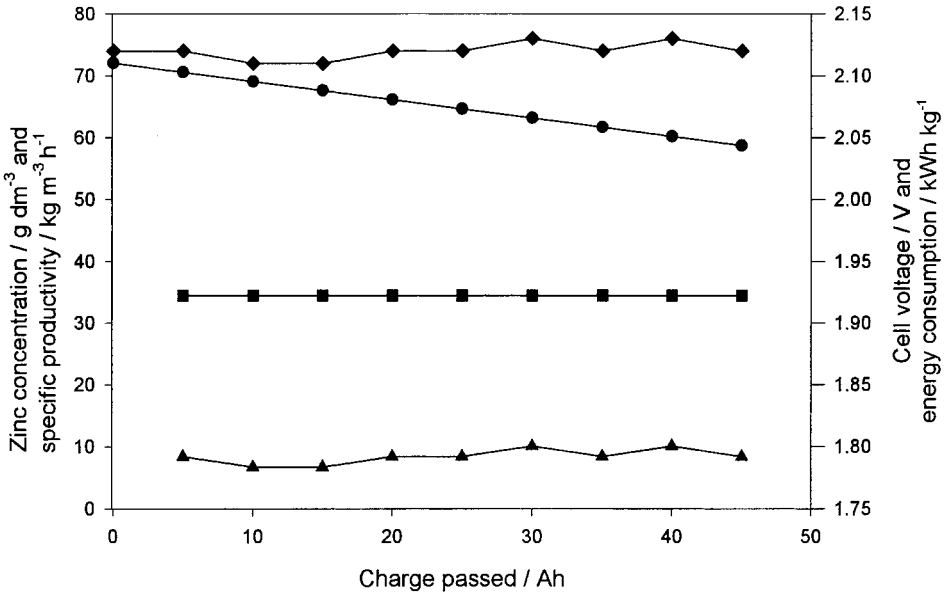

Fig. 11. Experiment with particles of mixed sizes, 72 g dm^{-3} zinc in 31.5 wt% KOH, anolyte 45 wt% KOH 1 dm^3, 40 °C, Daramic 0.25 mm, Aver. CE 97%, 1140 A m^{-2}. Key: (●) zinc concentration, (■) specific productivity, (◆) cell voltage and (▲) energy consumption.

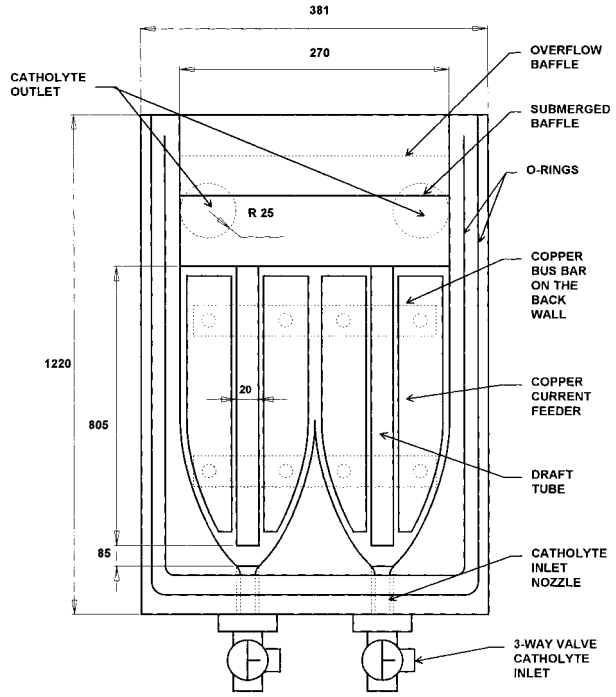

Fig. 12. Schematic of the large cell cathode compartment (view from anode side).

was brought up to temperature and the flow started. Once proper spouting was established the current was turned on and electrolysis proceeded until the cell was shut down.

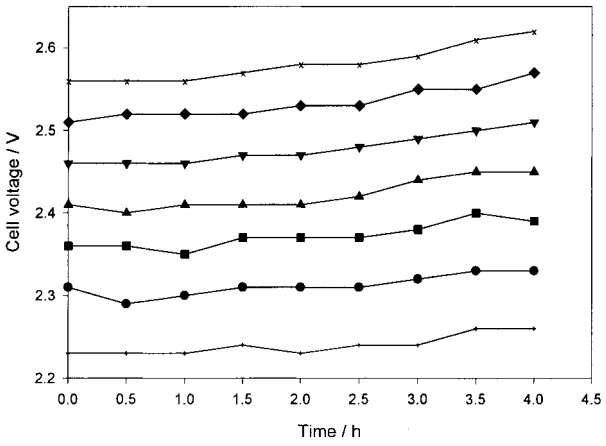

Fig. 13. Time dependence of cell voltage of the large cell at different current densities. Key: (×) 1333, (◆) 1666, (▼) 2000, (▲) 2333, (■) 2666, (●) 3000 and (+) 3333 in A m^{-2}.

3.2. *Experimental results*

The cell was operated to a controlled shut-down in all fifteen experimental runs. The only experimental difficulty encountered, deposition of metal on the diaphragm, was eliminated, once some imprecision in machining was corrected. Cell voltage and current, as well as electrolyte temperature were monitored during a run. As with the smaller cell, polarization curves were obtained by varying the cell current occasionally during a run. Figure 13 shows typical results; the cell voltage is

Table 1. Some details of the design for the large SBE zinc regeneration cell

Materials of construction	Cell structural parts	Plexiglas®
	Clamps, support frame, etc	Steel
	Current collectors	Copper
	Anode connections/supports	Stainless steel
	Piping and valves	PVC
Current collectors	Copper	
Anode	Electrolyser Corp. (Toronto)	
	NE-A-30	
Diaphragm	Pal RAI E40201 plus G.C.Processing, HS	
Dimensions	External height	1.22 m
	External width	0.381 m
	External thickness	0.094 m
	SBE height	0.889 m
	SBE width (overall)	0.27 m
	Draft tube length	0.804 m
	Draft tube width (outside)	20 mm
	Nozzle diameter	10 mm
	Nozzle-draft tube distance	25 mm
	Inclination of base	65°
	Anode/current collector dimensions	0.5 m × 0.23 m
Pump	50 dm^3 min^{-1}	
Tank	100 dm^3	
Electrolyte temperature control	Thermostated stainless steel electric immersion heaters in tanks with auxiliary stainless steel cooling coil operating on city water	
Power supply	0–1500 A, 0–100 V d.c. power supply	
Data acquisition	Strawberry Tree data acquisition board and PC	
Nominal cell current	175A (5 kg Zn per day) per module	
Nominal voltage	2.45 V	
Nominal energy consumption	2 kWh kg^{-1} zinc at 175 A	

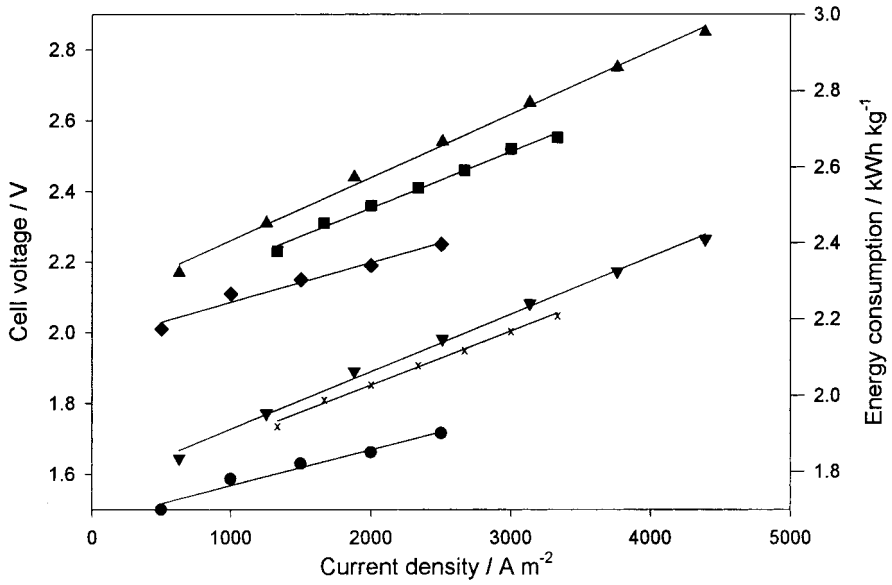

Fig. 14. Comparison of the cell voltage and energy consumption of three spouted bed cells at different current densities. Key: (◆, ●) small cell voltage and energy consumption, (▲, ▼) intermediate cell voltage and energy consumption and (■, ×) ZB2 cell voltage and energy consumption, respectively.

seen to hold nearly constant throughout a run, except towards the end of a run where some increase in voltage is probably due to electrolyte depletion.

Figure 14 compares the performance of the spouted bed electrode in this application at three scales. The smallest scale is that of the laboratory cell depicted in Figure 1 with a bed 95 mm wide and 178 mm high. The intermediate scale is a taller cell (120 mm by 360 mm) that was used in experiments on the Union Miniere particles (see above). The ZB2 cell (after the designation of the sponsors) is that (275 mm by 915 mm bed) shown in Figure 12. In the last case a representative 95% current efficiency (determined by weighing) was used in calculating energy consumption from cell voltages. The cell is seen to have been significantly scaled up without a major change in cell voltage and energy consumption. The slightly lower voltages for the small cell are a result of the Celgard diaphragm used in this early work. Celgard 5550 yielded the lowest voltage of the materials tried, although that voltage rose unacceptably in long term runs. It should be noted that the large cell was operated at a maximum current of 360 A, that is, more than twice the design current, without experimental difficulties.

4. Conclusion

This investigation has demonstrated that a spouted bed electrode can be used to regenerate particles from the spent electrolyte that would be produced by a zinc–air fuel cell. In most cases the energy consumption is low, typically below 2 kWh kg^{-1} zinc for current densities below 1500 A m^{-2}. Particles were grown from a 0.4 mm seed to a final size of 1 mm. (i.e., by a factor of about 17 by mass). The final particles exhibited some porosity.

Celgard 5550 appeared to be unsuitable for this application in long term experiments, due to a steady increase in cell voltage thought to be due to a loss of hydrophilic character. An alternative diaphragm material (a combination of two materials) was identified and shown to give a stable voltage.

A larger cell, designed to regenerate 5 kg of zinc in 24 h, was built and operated at up to twice the design current (up to 350 A). Cell voltages and energy consumptions (kWh kg^{-1} zinc) were comparable with those in smaller cells.

Acknowledgement

The authors are grateful for the support of this investigation by the International Lead–Zinc Research Organization.

References

1. F.G. Will, 'Recent Advances in Zinc/Air Batteries', Proceedings of the 13th Annual Battery Conference on Applications and Advances, Long Beach CA, Jan. 1998.
2. G. Savaskan and J.W. Evans, *J. Appl. Electrochem.* **21** (1991) 105–10.
3. G. Savaskan and J.W. Evans, Battery Using a Metal Particle Bed Electrode, *U.S. Patent 5 006 424* (Apr. 1991).
4. G. Savaskan, T. Huh and J.W. Evans, *J. Appl. Electrochem.* **22** (1992) 909–15.
5. J.C. Salas and J.W. Evans, *J. Appl. Electrochem.* **24** (1994) 858–62.
6. J.F. Cooper, 'Continuous-Feed Electrochemical Cell with Non-packing Particulate Electrode', *US Patent 5 434 020* (1995).
7. J.F. Cooper, D. Fleming, D. Hargrove, R. Koopman and K. Petennan, SAE Technical Paper Series (SP-1 105), Paper 951948 (1995), p. 137.
8. T. Huh, G. Savaskan and J. W. Evans, *J. Appl. Electrochem.* **22** (1992) 916–21.

9. J.C. Salas-Morales, PhD dissertation, University of California, Berkeley (1994).
10. J.C. Salas-Morales, J.W. Evans, O.M.G. Newman and P.A. Adcock, *Met. and Mat. Trans. B* **28** (1997) 59–68.
11. A. Verma, J.C. Salas-Morales, and J.W. Evans, *Met. and Mat. Trans. B* **28** (1997) 69–9.
12. F.J. Tamargo and Y. Lefevre, *in* T. Azakami, N. Masuko, J.E. Dutrizac and E.' Ozberk (Eds), 'Operational Results for the Latest Cellhouse Built by Asturiana de Zinc', Zinc & Lead '95, Min. Mater. Proc. Inst. Japan, Tokyo (1995), pp. 697–706.